Spectral, electrochemical and thermal characteristics of glass forming hydrazine derivatives

ARTICLE *in* OPTICAL MATERIALS · JULY 2014

Impact Factor: 1.98 · DOI: 10.1016/j.optmat.2014.07.013

8 AUTHORS, INCLUDING:

Malgorzata Wiacek

University of Silesia in Katowice

13 PUBLICATIONS **33** CITATIONS

SEE PROFILE

Jan Grzegorz Małecki

University of Silesia in Katowice

158 PUBLICATIONS **675** CITATIONS

SEE PROFILE

Ewa Schab-Balcerzak

Polish Academy of Sciences

110 PUBLICATIONS **862** CITATIONS

SEE PROFILE

Optical Materials 37 (2014) 498–510

Contents lists available at ScienceDirect

Optical Materials

journal homepage: www.elsevier.com/locate/optmat

Spectral, electrochemical and thermal characteristics of glass forming hydrazine derivatives

Katarzyna Bijak [a], Danuta Sek [b], Mariola Siwy [b], Marzena Grucela-Zajac [a], Henryk Janeczek [b], Malgorzata Wiacek [a], Grzegorz Malecki [a], Ewa Schab-Balcerzak [a,b,*]

[a] Institute of Chemistry, University of Silesia, 9 Szkolna Str., 40-006 Katowice, Poland
[b] Centre of Polymer and Carbon Materials, Polish Academy of Sciences, 34 M. Curie-Sklodowska Str., 41-819 Zabrze, Poland

ARTICLE INFO

Article history:
Received 14 February 2014
Received in revised form 9 July 2014
Accepted 11 July 2014
Available online 13 August 2014

Keywords:
Azines
Molecular glasses
Photoluminescence
Electrochemistry
DFT calculation

ABSTRACT

The azines being condensation products of benzophenone hydrazone with triphenylamine substituted with different numbers of aldehyde groups and also with terephthaldicarboxaldehyde were prepared. Their spectral, thermal and electronic properties that is, orbital energies and resulting energy gap calculated theoretically by density functional theory (DFT) and estimated by electrochemical measurements were explored. The prepared hydrazine derivatives exhibited glass-forming properties with glass-transition temperatures in the range of 10–98 °C and high thermal stability with decomposition temperatures placed between 231 and 337 °C. The photoluminescence (PL) studies showed that all investigated compounds both in solid state as blends with PMMA and in NMP solution emitted blue light, however, with different intensity. Relative PL intensity of azines was investigated in NMP in relation to rhodamine-B used as a standard. Moreover, the stability of azines during doping with acid and ferric chloride was spectroscopically demonstrated via repeated doping/dedoping in solution and in film. All compounds are electrochemically active. Depend on chemical structure of azines they undergo reversible or irreversible electrochemical oxidation and reduction processes. The LUMO levels were found in the range from −2.66 to −3.0 eV. They exhibited energy band gap (E_g) estimated electrochemically from 2.57 to 3.22 eV.

1. Introduction

The development of organic materials, both low molecular weight compounds and polymers, is the subject of recent research in the area of photonics and electronics. The important advantages of organic compounds are light-weight, good processability and tunability of their properties by structure modifications [1,2]. Significant advances have been reached in the field of organic electronics and optoelectronics based on low molecular weight compounds [3]. Small molecules in relation to polymers have advantages such as well-defined structure and molecular weight without any distribution, easier purification and more easily controllable properties. However, active layers in devices for organic electronics based on molecular materials are usually obtained by evaporation, thus limiting their use [3]. Thus, especially interesting are low molecular weight compounds that readily form glasses above room temperature which are called molecular glasses or amorphous molecular materials [4–8]. They combine the characteristic properties of small molecules with behavior of polymers, that is, the ability to access amorphous solid states. They may form uniform, transparent amorphous thin films by spin-coating methods contrary to low molar mass compounds with strong tendency for crystallization.

Organic azines (diimines) belong to a group of π-conjugated compounds, which seem to be promising for organic (opto)electronics. However, taking into account the literature review concerns aiznes it can be concluded that, they are rather seldom investigated for optoelectronic applications. They have been usually widely studied because of their numerous chemical and biological applications [9–11]. To the best of our knowledge, there are a few articles in which azines are proposed for applications in optoelectronic devices [12–18]: as potential nonlinear optical (NLO) materials [12–14], as liquid crystals [13,15] also as thermoluminescent materials [15] and as thermochromic compounds [16,17]. It should be mentioned that principal role with respect to NLO properties plays intramolecular charge transfer from the donor to the acceptor due to molecule became polarized [18]. Considering various π-spaces, that is, vinylene, azine, arylimine

* Corresponding author at: Centre of Polymer and Carbon Materials PAS, 34 M. Curie-Sklodowska Str., 41-819 Zabrze, Poland.
E-mail address: ewa.schab-balcerzak@us.edu.pl (E. Schab-Balcerzak).

http://dx.doi.org/10.1016/j.optmat.2014.07.013
0925-3467/

and ethynylene it was found that vinylene and azine have the more favorable effect on the absorption spectrum and redox properties [19]. Thus, azines seem to be promising compounds for optoelectronic devices. Inspired by the findings described above we have undertaken a preparation and investigation of four aromatic azines obtained from benzophenone hydrazone and one prepared from benzophenone and hydrazine. Considering chemical structure of these azines there is a one example of the same compounds in literature [20]. A synthesis of azine, described in this paper, that is, prepared from benzophenone and hydrazine has been reported [20]. However, such diimine was obtained from differ substrates than in our case, that is, in solvent-free resection of benzophenone hydrazone with benzophenone using sulfated titania as catalytic system [20]. The aim of mentioned work was to develop a simple method under mild conditions for the preparation of azines. Three azines described in this paper contain triphenylamine group (TPA), which is well-known for its hole-transporting properties. Low molecular weight compounds and polymers with triarylamine units are also expected to exhibit good solubility, stability and high photoluminescence efficiency and are therefore widely investigated as materials for organic light emitting diodes, solar cells and organic field-effect transistors [21–23]. Symmetrical azine obtained from hydrazine and 4-formyltriphenylamine has been described in literature, including our previous work [19,24,25]. This compound has proved to be convenient chromogenic sensor for the detection of mercury ions [24]. The azine forms molecular glass, which allows preparing uniform transparent thin films of the compound using spin-coating techniques [25]. Its optical and electrochemical properties have been examined [19,25] and compared with azomethine analogue [25] and azine with carbazole end-groups [19].

The nitrogen atom in imine linkages has lone pair electrons. It can form intra or inter molecular interactions, conduct protonation and complexation with metal ions, acids and iodine [26]. Therefore, compounds may possess novel optical properties because both absorption and photoluminescence can be modulated by chemical environment. The research described in this work is the continuation of our efforts in the search of organic materials both polymers and low molecular weight compounds and for applications in organic (opto)electronics [25,27–33].

This paper describes the synthesis and thermal (DSC, TGA) and optical (UV–Vis, PL) and electrochemical properties of four new symmetrical and unsymmetrical azines synthesized from benzophenone hydrazone and one obtained from benzophenone and hydrazine. Additionally, the electronic properties of obtained compounds are described theoretically by density functional theory (DFT).

2. Experimental

2.1. Materials

4-Formyltriphenylamine, 4,4′-diformyltriphenylamine, tris (4-formylphenyl)amine, benzophenone hydrazone, hydrazine monohydrate (80% solution), trifluoroacetic acid, terephthaldicarboxaldehyde and *N*-methyl-2-pyrrolidone (NMP) were obtained from Aldrich. Ethanol and toluene were supplied from POCh.

2.2. Synthesis of azines (***AHs***)

2.2.1. Synthesis of ***AH-1***

4-Formyltriphenylamine (0.1367 g, 0.5 mmol) and benzophenone hydrazone (0.0981 g, 0.5 mmol) were dissolved in 5 ml ethanol and 2 drops of trifluoroacetic acid were added. The reaction mixture was stirred for 24 h at 80 °C and cooled to room temperature. The resulting precipitate was filtered, washed with hot ethanol and dried.

AH-1: Yellow powder. Yield: 29%. Elem. anal.: found(calcd)% C 84.62(85.11), H 5.50(5.58), N 9.67(9.31). ^{1}H NMR ($CDCl_3$, δ, ppm): 8.57–8.52 (d, —CH═N, 1H), 7.68 (d, 2H), 7.34–7.28 (m, 8H), 7.17–7.06 (m, 14H). ^{13}C NMR ($CDCl_3$, δ, ppm): 161.09 (—CH═N), 150.46, 147.13, 129.61, 127.49, 125.55, 124.10, 121.84. FTIR (cm^{-1}): 3061, 3035 (CH aromatic), 1617 (CH═N stretching), 1591 (C═C stretching deformations in phenyl ring).

2.2.2. Synthesis of ***AH-2***

4,4′-Diformyltriphenylamine (0.1506 g, 0.5 mmol) and benzophenone hydrazone (0.1962 g, 1 mmol) were dissolved in 5 ml ethanol and 2 drops of trifluoroacetic acid were added. The reaction mixture was stirred for 24 h at 80 °C and cooled to room temperature. The resulting precipitate was filtered, washed with hot ethanol and dried.

AH-2: Yellow powder. Yield: 45%. Elem. anal.: found (calcd)% C 83.08(83.99), H 5.22(5.36), N 11.02(10.65). ^{1}H NMR ($CDCl_3$, δ, ppm): 8.52–8.609 (m, —CH═N, 2H), 7.75–7.72 (m, 5H), 7.56 (m, 3H), 7.46–7.31 (m, 16H), 7.19–7.05 (m, 9H). ^{13}C NMR ($CDCl_3$, δ, ppm): 161.12 (—CH═N), 159.20 (—CH═N), 149.50, 146.49, 138.58, 135.69, 130.56, 130.30, 129.80, 129.25, 128.99, 128.36, 127.65, 126.23, 124.90, 123.31. FTIR (cm^{-1}): 3055, 3026 (CH aromatic), 1620 (CH═N stretching), 1594 (C═C stretching deformations in phenyl ring).

2.2.3. Synthesis of ***AH-3***

Tris(4-formylphenyl)amine (0.1647 g, 0.5 mmol) and benzophenone hydrazone (0.2944 g, 1.5 mmol) were dissolved in 5 ml ethanol and 2 drops of trifluoroacetic acid were added. The reaction mixture was stirred for 24 h at 80 °C and cooled to room temperature. The resulting precipitate was filtered, washed with hot ethanol and dried.

AH-3: Yellow powder. Yield: 52%. Elem. anal.: found(calcd)% C 83.61(83.40), H 5.18(5.25), N 11.36(11.35). ^{1}H NMR ($CDCl_3$, δ, ppm): 8.51–8.63 (m, —CH═N, 3H), 7.75–7.71 (m, 6H), 7.56 (m, 4H), 7.48–7.28 (m, 24H), 7.22–7.05 (m, 8H). ^{13}C NMR ($CDCl_3$, δ, ppm): 160.67 (—CH═N), 158.99 (—CH═N), 138.33, 135.52, 130.55, 129.73, 129.47, 129.29, 128.81, 128.39, 128.16, 128.01, 127.68, 124.38. FTIR (cm^{-1}): 3049, 3022 (CH aromatic), 1619 (CH═N stretching), 1594 (C═C stretching deformations in phenyl ring).

2.2.4. Synthesis of ***AH-4***

4 mmol (0.729 g) of benzophenone dissolved in 5 ml of toluene at room temp. and then solution of 2 mmol (0.1001 g)of hydrazine in 3 ml toluene was added dropwise and then 3 drops of acetic acid was added. This solution was heating to 110 °C under argon atmosphere. The reaction mixture was stirred for 28 h at 110 °C. This mixture was cooled to room temperature and precipitate was separated.

AH-4: White powder. Yield: 34.7%. Elem. anal.: found(calcd)% C 86.50(86.63), H 6.02(5.59), N 7.50(7.72). ^{1}H NMR ($CDCl_3$, δ, ppm): 7.48–7.46 (m, 4H), 7.41–7.36 (m, 4H), 7.34–7.31 (m, 8H), 7.30–7.28 (m, 4H). ^{13}C NMR ($CDCl_3$, δ, ppm): 158.91 (C═N), 129.73, 129.50, 128.81, 128.16, 128.01. FTIR (cm^{-1}): 3083–3023 (CH aromatic), 1587 (C═C stretching deformations in phenyl ring).

2.2.5. Synthesis of ***AH-5***

0.5 mmol (0.068 g) of terephthaldicarboxaldehyde and 1.5 mmol (0.2944 g) of benzophenone hydrazone dissolved in 5 ml ethanol. After few minutes yellow product started to precipitate. The reaction mixture was stirred for 5 h at room temperature under argon atmosphere. The precipitate was filtered, washed several times with ethanol and dried at 60 °C in vacuum.

AH-5: Yellow powder. Yield: 88%. Elem. anal.: found(calcd)% C 83.62(83.23), H 5.28(5.34), N 11.54(11.62). ^{1}H NMR ($CDCl_3$, δ, ppm): 8.56 (s, —CH═N, 2H), 7.71 (m, 4H), 7.65 (s, 4H), 7.45–7.35 (m, 12H), 7.34–7.33 (m, 4H). ^{13}C NMR ($CDCl_3$, δ, ppm): 158.76 (—CH═N), 138.33, 136.84, 135.43, 130.53, 129.35, 129.21, 128.82, 128.41, 127.73. FTIR (cm^{-1}): 3084–3026 (CH aromatic), 1601 (CH═N stretching).

2.3. Blend and film preparation

Blends were obtained by dissolving the desired amount of compounds and PMMA in NMP to form a homogeneous solution. Films cast on glass were dried in vacuum oven at 90 °C over 10 h. Thin films were prepared from dissolved compound in dichloromethane (10^{-5} M) spin coated on glass substrate at 1500 rpm for 20 s.

2.4. Measurements

^{1}H NMR and ^{13}C NMR spectroscopy were carried out on a Avance II Ultra Shield Plus BRUKER 600 MHz Spectrometer using $CDCl_3$ as solvent and TMS as the internal standard. FTIR spectra were recorded on a Spectrum One Spectrometer (Perkin Elmer) with spectral resolution 0.01 nm using KBr pellets. Elemental analyses were performed using a Vario EL III apparatus (Elementar, Germany). Differential scanning calorimetry (DSC) was performed with a TA-DSC 2010 apparatus (TA Instruments, Newcastle, DE, USA) accuracy 0.1 °C, under nitrogen using aluminum sample pans. Thermogravimetric analyses (TGA) were performed on a Perkin Elmer apparatus at heating rate of 10 °C/min under nitrogen (accuracy 0.01 mg). UV–vis absorption spectra were recorded using a Lambda Bio 40 Perkin Elmer spectrophotometer with spectral resolution 0.1 nm. The PL spectra were obtained on a VARIAN Cary Eclipse Fluorescence Spectrophotometer with spectral resolution 2 nm. Electrochemical measurements were carried out using Jaissle IMP 83 PC T-BC potentiostat (accuracy 10 μA). Cyclic voltammetry experiments were conducted in a standard one compartment cell, in MeCN (Fluka, HPLC grade). 0.1 M tetrabutylammonium hexafluorophosphate (Bu_4NPF_6 Aldrich, 99%) was used as the supporting electrolyte. The oxidation and reduction potentials of film coated on a ITO disk were measured using a Pt wire and a Ag/AgCl electrode as a counter electrode and a quasi reference electrode, respectively. Potentials were referenced with respect to ferrocene (Fc), which was used as the internal standard. The HOMO and LUMO levels were calculated by assuming the absolute energy level of Fc/Fc + as −4.82 eV to vacuum.

3. Result and discussion

In the article the synthesis and characterization of compounds being condensation products of benzophenone hydrazone with triphenylamine (TPA) substituted with different numbers of aldehyde groups and also with terephthaldicarboxaldehyde are described from point of view of their spectral, thermal and HOMO and LUMO energy levels practically and theoretically calculated by density functional theory (DFT).

The chemical structures of obtained compounds which were soluble in many organic solvents except for **AH-3** (Table 1) are presented in Fig. 1.

Instrumental technique including FTIR, ^{1}H NMR, ^{13}C NMR spectroscopies were applied for the characterization of the molecular structure of the compounds. The absence of the residual amino (NH_2) and aldehyde (CHO) groups together with the appearance of a band typical for imine bonds (HC═N—) was confirmed by NMR and FTIR spectra. In the ^{1}H NMR spectra of the hydrazine derivatives, except the **AH-4**, the imine proton signal was observed in the range of 8.52–8.63 ppm. However, it should to be stressed that only in the compound **AH-5** being the condensation of benzophenone hydrazone and terephtalaldehyde, the imine proton signal was detected as a singlet. In the case of the others compounds the imine proton signals were spitted. For the compound **AH-1** two signals at 8.52 ppm and 8.57 ppm were observed. In the case of the compound **AH-2** those two signals were spitted and were seen at 8.52 ppm and 8.53 ppm and between 8.58 ppm and 8.60 ppm as a quartet. For the compound **AH-3** the following signal of the imine proton was observed; between 8.51 ppm and 8.55 ppm quartet was found and between 8.59 ppm and 8.63 ppm six signals were present. Fig. 1S in Supporting Information shows the ^{1}H NMR spectra of the compounds **AH-1**, **AH-2** and **AH-3** in the region of 8.4–8.65 ppm. It is interesting that the area ratio of the signals at higher and lower fields increased in dependence of the amounts of the imine units in the molecules and was found to be 0.046 for the compound **AH-1,** 1.582 for the **AH-2** and 6.382 for **AH-3**. The splitting of the signals seems to confirm the presence of various isomers and conformers in these compounds. This phenomenon needs additional investigations (measurements in different solvents and different temperatures) to be explained in details, however, such study are out of the scope of this paper and will not be carried out in this work. The signals of the imine hydrogen atom in the compounds **AH-1**, **AH-2** and **AH-3** at higher field were observed in the same position while those present at lower field were little downfield shifted if one considers the compound from **AH-1** to **AH-3**. In ^{13}C NMR spectra of the compounds **AH-1** – **AH-3** and **AH-5** the signal in the range of 158.7–161.1 ppm confirmed the existence of carbon atom in the imine group. In FTIR spectra of the investigated compounds the bands characteristic for the CH═N stretching vibration were detected in the range of 1601–1620 cm^{-1}. From the literature data it follows that a free, isolated C═N group absorbs at about 1660 cm^{-1} and this band is associated with the stretching vibrations of this group [34]. The frequency of this band is strongly reduced with conjugation of the C═N group with phenyl ring due to diminishing of the energy of the C═N bond and delocalization of nitrogen pair into imine double bond. The exact position of this band in AHs varies up to 19 cm^{-1} and is shifted towards lower wavenumbers for the compound obtained from terephthaldicarboxaldehyde (**AH-5**). The lower wavenumber of the imine group absorption indicates the better conjugation of π-electrons with phenyl ring π-electrons. The wavelength number value of the imine absorption of the others azines is in the similar range. Additionally, their structures were confirmed by elemental analysis, which showed very good agreement of the calculated and found content of carbon, nitrogen and hydrogen in the compounds (cf. Section 2).

Table 1
Solubility behavior of the obtained compounds.

Code	Solvent							
	$CHCl_3$	THF	CH_2Cl_2	Acetone	CH_3OH	NMP	CH_3CN	DMSO
AH-1	++	++	++	±	±	+	±	+
AH-2	++	++	++	±	±	++	±	+
AH-3	±	±	±	±	±	±	±	±
AH-4	++	++	++	++	+	++	+	+
AH-5	++	++	++	±	±	++	+	+

The qualitative solubility was tested by dissolving 2.5 mg samples in 1 ml of solvent; ++ soluble at room temperature, + soluble after heating, ± partially soluble after heating.

3.1. Thermal properties

Differential scanning calorimetry (DSC) and thermogravimetric analysis (TGA) in nitrogen atmosphere were utilized to examine

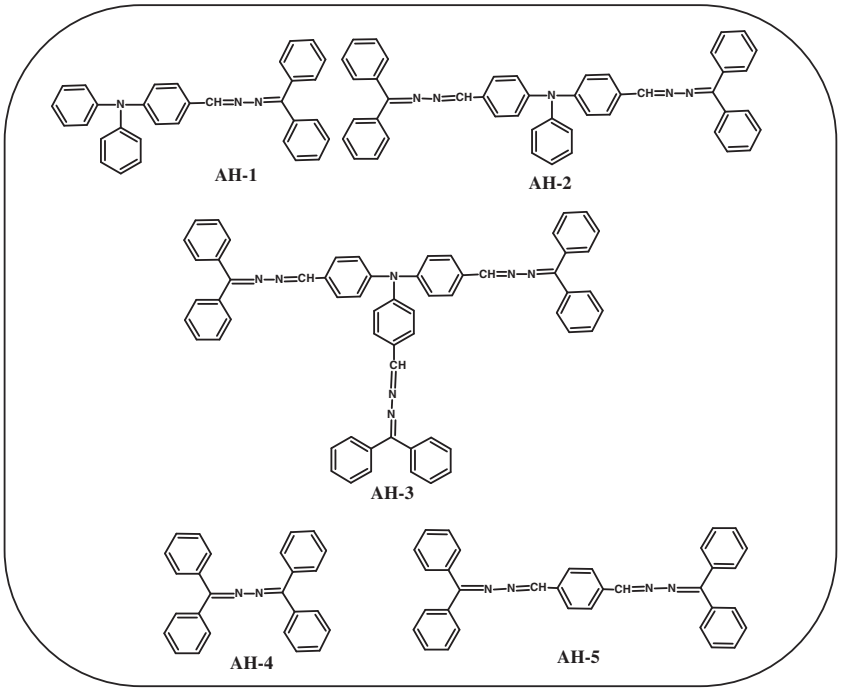

Fig. 1. Chemical structures of investigated compounds.

thermal properties of the obtained azines. It is clear that thermal properties of the compounds depend strongly on their chemical structure and different behavior of hydrazine derivatives was found. Thermal properties of investigated compounds are collected in Table 2.

Formation of the glassy state of obtained hydrazine derivatives was investigated by DSC. The first and the second run heating scans of the investigated compounds were carried out with heating rate 20 °C/min. The second heating was recorded immediately after a rapid cooling. Fig. 2. presents as a example the DSC thermogram of AH-1.

DSC thermogram of the compounds AH-1, AH-4 and AH-5 during first heating run showed one endotherm at 238, 165 and 198 °C indicating melting of the sample. After rapid cooling, during the second heating run, glass transition (T_g), "cold" crystallization (exothermic peak) at 119, 60 and 93 °C, and a melting endotherm at 237, 164 and 197 °C for AH-1, AH-4 and AH-5 were detected, respectively. In the case of symmetrical azines with TPA structure, that is, AH-2 and AH-3 the first heating scan revealed T_g at 98 and 64 °C, respectively, and during the second heating these samples exhibited only glass transition, which temperatures are collected in Table 2. Thus, all obtained azines are molecular glasses. However, they differ in value of T_g and the highest exhibited compounds with TPA units and at the same time the presence of

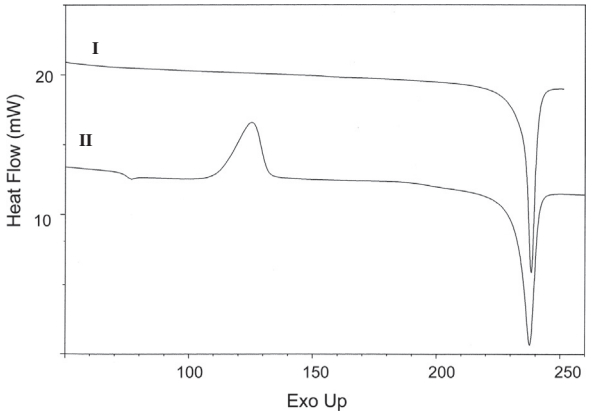

Fig. 2. DSC scans of azine AH-1: where (I) first heating run (20 °C/min), (II) second heating run (20 °C/min) after rapid cooling.

three TPA units lower T_g in relation to one and two TPA moieties in compound.

The thermal stability of obtained hydrazone derivatives was evaluated on the basis of TGA analysis. The temperatures at 5% and 10% weight loss (T_5, T_{10}), temperature of maximum decomposition

Table 2
Thermal data of investigated compounds.

Code	T_5[a] (°C)	T_{10}[a] (°C)	T_{max}[b] (°C)	Residual weight[c] (%)	T_g[d] (°C)
AH-1	337	350	364 (I step) 428 (II step)	5.4	74
AH-2	325	340	360	26.5	98
AH-3	260	285	298 (I step) 375 (II step) 592 (III step)	33.0	64
AH-4	231	261	330	0	10
AH-5	325	335	354	7.1	47

[a] T_5, T_{10}: temperatures at 5%, 10% weight loss, respectively.
[b] Temperature of maximum decomposition rate.
[c] Residual weight when heated to 800 °C in nitrogen.
[d] T_g detected in second DSC heating scan.

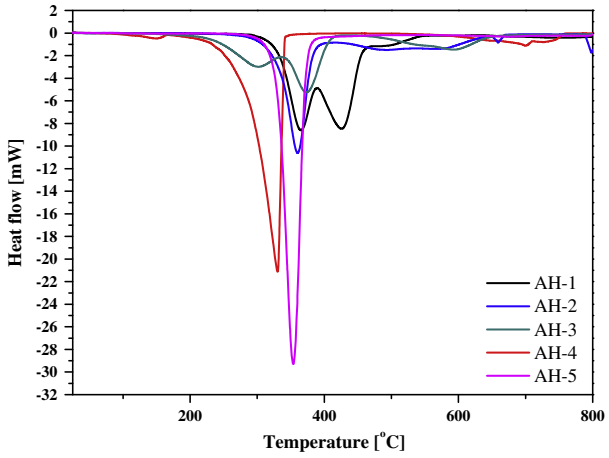

Fig. 3. DTG curves of investigated azines.

rate (T_{max}) and residual weight at the end of experiment were determined (Table 2). The dynamic thermogravimetric (DTG) curves of the azines are shown in Fig. 3.

The thermal decomposition proceeded through one or two or three steps depend on compound structure. The 5% and 10% weight loss temperature, which is usually considered as the criterion for determining the thermal stability decrease together with increase of number of imine linkages in compounds with TPA units and the same concerns T_{max}, as evidenced by the DTG curves. On the other hand considering residual weight of sample at 800 °C reverse tendencies were found, that is, along with increase number of imine groups and aromatic rings increase amount of char yield was observed. As can be expected the lowest thermal stability showed compound with the lowest number of aromatic rings (AH-4).

3.2. Optical properties of azines

Spectral properties of prepared hydrazine derivatives were analyzed by UV–vis and photoluminescence (PL) measurements in solvents exhibiting different dielectric constants (ε) such as $CHCl_3$ (4.8), THF (7.6), CH_2Cl_2 (8.9), NMP (33) and DMSO (46.7) and also in solid state as thin film on glass substrate and as a blend with nonemissive poly(methyl methacrylate) (PMMA). Dispersed luminescent compound in nonemissive polymer matrix let to eliminate the self-quenching of fluorescence due to the dilution effect [35,36]. Polymer blends involving luminescent compound and inert polymer as matrices are often used in polymer light emitting diodes as a tool to increase the efficiency of the devices [35,37]. It should be stressed that obtained compounds contain specific sites needed to construct supramolecules and azines with TPA structure have two kinds of basic nitrogen atoms which can be doped. It was found that imines are readily protonated [38]. As doping agent HCl, and for chosen compounds trifluoroacetic acid (TFA) and ferric chloride ($FeCl_3$) were applied. Moreover, reversibility of doping process was investigated.

3.2.1. Ultraviolet–visible investigations

The UV–vis absorption data are collected in Table 3 and UV–vis spectra are showed in Fig. 4 and in Fig. 2S in Supporting Information.

Absorption spectra of the investigated compounds showed similar characteristics in all solvents and exhibited two absorption bands: one with the position of the absorption maximum (λ_{max}) in the range of 276–305 nm being responsible for n-π transition in aromatic rings and the second having λ_{max} in the range of 313–422 nm which attributed to the π–π* transition in the imine group. However, in the case of compounds without triphenylamine structures (AH-4 and AH-5) λ_{max} from lower energy region was significantly hypsochromically shifted. Considering the influence of the dielectric constant of the solvent on λ_{max}, the solvatochromism was not observed (cf. Table 3 and Fig. 2S in Supporting Information). For the hydrazine derivatives with TPA units absorption band in blends are hypsochromically shifted in comparison with the ones in NMP solution. In the case of AH-4 and AH-5 opposite tendency was observed, that is, λ_{max} in blends is shifted into lower energy region. It was found that absorption properties of azine with TPA unit (AH-1) in film are the same as in solution (cf. Fig. 4b). Whereas in the case of AH-5 bathochromic shift in λ_{max} in film compare to solution was observed (cf. Table 3).

3.2.2. Photoluminescence investigations

Emission spectra of the compounds were investigated under various both excitation wavelengths (λ_{ex}) and kind of solvent. The results of the study are collected in Table 4 and Fig. 5 presents the representative PL spectra.

Photoluminescence properties of all azines were studied in NMP and $CHCl_3$ solutions and for the compounds **AH-1** – **AH-3** THF and DMSO were also used as solvents and in the case of **AH-1** and **AH-5** also dichloromethane was utilized (cf. Fig. 3S in Supporting Information). The highest emission intensity was observed in NMP solution for all compounds. The emission in $CHCl_3$ and CH_2Cl_2 solution

Table 3
The results of UV–vis measurements of studied compounds in different solvents ($c = 1 \times 10^{-5}$ mol/l) and in solid state as blends with PMMA and thin film.

Code	$CHCl_3$ (ε = 4.81)[a]		THF (ε = 7.58)[a]		CH_2Cl_2 (ε = 8.9)[a]		NMP (ε = 33.00)[a]		DMSO (ε = 46.70)[a]		Blend[b]	Film
	λ_{max} (nm)	ε (l mol^{-1} cm^{-1})	λ_{max} (nm)	ε (l mol^{-1} cm^{-1})	λ_{max} (nm)	ε (l mol^{-1} cm^{-1})	λ_{max} (nm)	ε (l mol^{-1} cm^{-1})	λ_{max} (nm)	ε (l mol^{-1} cm^{-1})	λ_{max} (nm)	λ_{max} (nm)
AH-1	296	22,280	293	17 580	295	23,080	293	15,700	296[c]	–	405	406
	407	50,840	401	34,850	404	49,670	404	58,660	404[c]	–		
AH-2	286	30,640	282	43,620	nd	nd	295	40,680	284	28,410	392[d]	nd
	420	60,690	414	81,820			419	70,850	420	65,220		
AH-3	282[c]	–	277[c]	–	nd	nd	305[c]	–	276[c]	–	410	nd
	419[c]	–	417[c]	–			422[c]	–	416[c]	–		
AH-4	279	24 490	nd*	nd	nd	nd	279	20,800	nd	nd	380[d]	nd
	313	18,080					317	14,930				
AH-5	351	50,540	nd	nd	349	44,560	351	41,410	nd	nd	368[d]	360

[a] ε: Dielectric constant.
[b] Blend with PMMA, concentration = 1% of compound in blend.
[c] Qualitative measurement.
[d] The position of absorption band calculated using the second derivative method (i.e., the minimum of the second derivative of absorption corresponds to the absorption maximum) and for such band ε was not calculated.
* Not determined.

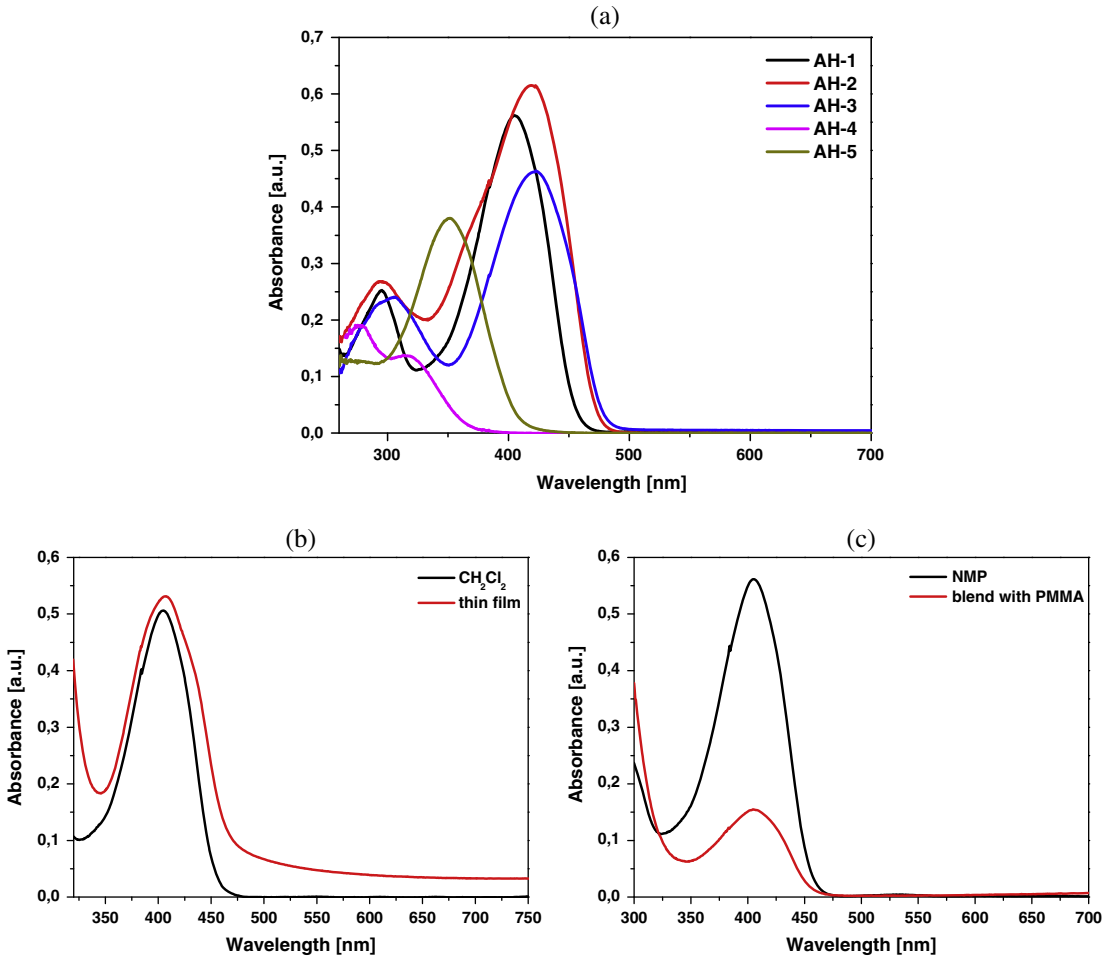

Fig. 4. UV–Vis absorption spectra (a) of investigated compounds in NMP solution ($c = 1 \times 10^{-5}$ mol/l; in the case of **AH-3** qualitative measurements), (b) of **AH-1** in CH_2Cl_2 solution and as thin film on glass substrate and (c) of **AH-1** in NMP solution and in blend with PMMA.

Table 4
The photoluminescence data of studied compounds under various excitation wavelengths, solvents and in solid state.

Code	Medium	PL λ_{em} (nm) λex (nm)					
		340	**350**	**360**	**420**	**440**	**450**
AH-1	$CHCl_3$[a]	484	479	478	486	**492**	488
	CH_2Cl_2[a]	488	**488**	488	–	–	–
	THF[a]	470	**472**	476	–	–	–
	NMP[a]	**466**	468	472	480	–	–
	Blend[b]	425	**431**	442	nd[*]	nd	nd
	Film	**498; 458**	462	465	467	nd	nd
AH-2	$CHCl_3$[a]	–	–	–	484	482	**482**
	NMP[a]	477	**477**	481	486	490	488
	Blend[b]	**441**	442	442	nd	nd	nd
AH-3	$CHCl_3$[c]	–	–	–	487	484	**491**
	NMP[c]	482	481	**483**	487	490	486
	Blend[b]	448	450	**445**	nd	nd	nd
AH–4	NMP[a]	474	472	**476**	479	–	–
	Blend[b]	**405; 432**	406; 432	417; 438	nd	nd	nd
AH-5	NMP[a]	471	474	**478**	478	–	–
	Blend[b]	**415**	449	460	493	nd	nd
	Film	**395**	427	439	465	nd	nd

Bold data indicates the most intense luminescence of compound.
[a] $c = 1 \times 10^{-5}$ mol/l.
[b] Concentration = 1% of compound in PMMA.
[c] Qualitative measurement.
[*] Not determined.

was observed only for the compounds containing TPA units (**AH-1** – **AH-3**). However, the intensity was very low in these solvents. Very weak emission was also observed in DMSO and THF solutions (except for **AH-1** in THF). In case of compound **AH-1** the influence of the solvent polarity on position of the emission band maximum (λ_{em}) was found (cf. Table 4). It was found that excitation wavelength influenced the emission spectra, that is, position of the emission band maximum (λ_{em}) and its intensity. In NMP solutions longer excitation wavelength shifted slightly bathochromically emission bands. The weakest emission was observed under λ_{ex} = 420, 440 and 450 nm for all compounds in NMP and for **AH-1** in THF. The opposite tendency was observed in $CHCl_3$, that is compounds **AH-1** to **AH-3** showed the highest emission under λ_{ex} = 440 or 450 nm. For the compounds with triphenylamine units, the highest emission intensity in NMP solution was observed after excitation with longer wavelength going from the compound **AH-1** to **AH-3** being 340 nm, 350 nm and 360 nm respectively. The similar relationship was found in $CHCl_3$ solution. The compound **AH-1** emitted light with highest intensity under λ_{ex} = 440 nm, whereas for the compounds **AH-2** and **AH-3** the highest emission intensity was observed under λ_{ex} = 450 nm. In the case of the compound **AH-4** and **AH-5** the highest intensity was found under λ_{ex} = 360 nm independent of the compound structure. In Fig. 5a relationship between λ_{ex} and PL intensity for the compound **AH-2** in NMP solution are presented as an example. If the chemical structure of the compounds was considered it could be seen that the λ_{em} in NMP solutions were

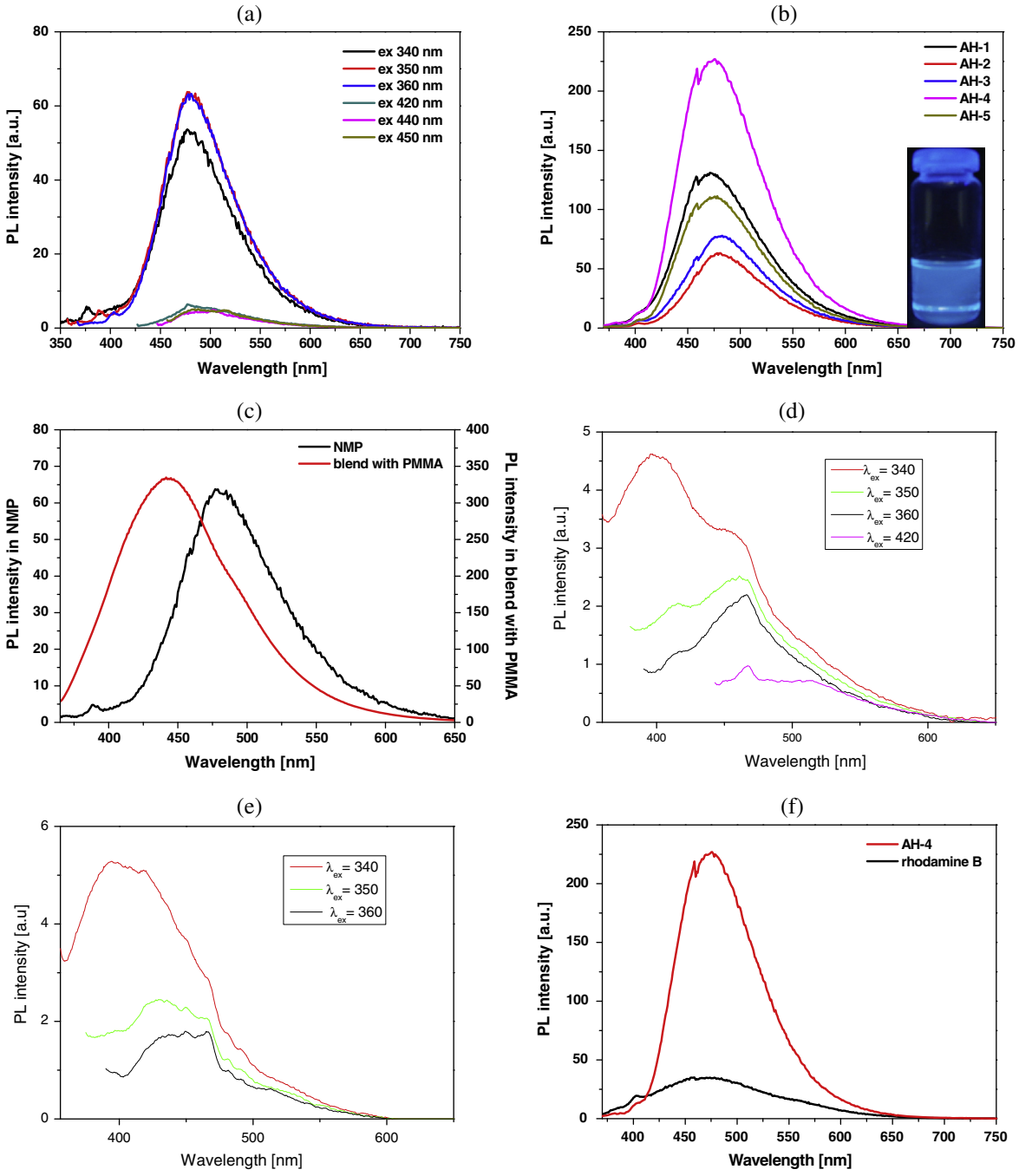

Fig. 5. PL spectra of (a) **AH-2** in NMP solution under various excitation wavelengths, (b) all investigated compounds under λ_{ex} = 360 nm, (c) **AH-2** under λ_{ex} = 350 nm in solution and in blend with PMMA (c = 1%), (d) AH-1 in film, (e) AH-5 in film and (f) PL relative intensity of **AH-4** under λ_{ex} = 360 nm in relation to rhodamine B in NMP ($c = 1 \times 10^{-5}$ mol/l).

shifted into the lower energy region when the amount of CH=N groups increased i.e. from the compound **AH-1** to **AH-3**. In $CHCl_3$ solutions such effect was not observed. Replacement of the triphenylamine moiety in the molecule core (**AH-2**) with 1,4-phenylene unit in **AH-5** caused hypsochromic shift of the emission band. The PL spectra of azines in NMP solution are compared in Fig. 5b. As was mentioned photoluminescence was also investigated for the compounds in solid state that means blended with nonemissive PMMA. As it can be seen in Table 4 emission bands detected in the

Table 5
The Stokes shifts values considering the most intensive emission band in each medium.

Medium	Stokes shifts (cm^{-1})				
	AH-1	**AH-2**	**AH-3**	**AH-4**	**AH-5**
NMP	3293	2902	2993	10537	7570
NMP + HCl	8911	5963	5325	10429	10835
Blend	1490	2834	1918	1624	3078
Blend + HCl	6166	4439	4321	5345	6198

Table 6
The position of λ_{max} of studied compounds after doping and dedoping.

Code	NMP + HCl	Blend + HCl[a]	CH_2Cl_2 + TFA	CH_2Cl_2 + TFA + Et_3N	CH_2Cl_2 + $FeCl_3$	CH_2Cl_2 + $FeCl_3$ + N_2H_4	Film + TFA	Film + TFA + Et_3N	Film + $FeCl_3$
AH-1	291; 353	343; 499	294; 406; 498	295; 404	310; 354; 532	294; 404	422; 531	416	416; 517
AH-2	297; 378	366; 495	nd*	nd	nd	nd	nd	nd	nd
AH-3	292; 374	369; 504	nd	nd	nd	nd	nd	nd	nd
AH-4	294	341[b]	nd	nd	nd	nd	nd	nd	nd
AH-5	291	342[b]	349	349	319; 364; 405	349	nd	nd	nd

[a] Blend with PMMA, concentration = 1% of compound in blend.
[b] The position of absorption band calculated using the second derivative method (i.e., the minimum of the second derivative of absorption corresponds to the absorption maximum) and for such band ε was not calculated.
* Not determined.

Table 7
The photoluminescence data of studied compounds after doping under various excitation wavelengths.

Code	Medium	PL λ_{em} (nm) λ_{ex} (nm)					
		340	**350**	**360**	**420**	**440**	**450**
AH-1	NMP + HCl[a]	515	**515**	516	518	531	531
	Blend + HCl[b]	430	nd	**435**	nd	nd	nd
	CH_2Cl_2 + TFA[a]	485	**487**	487	–	635	635
	CH_2Cl_2 + $FeCl_3$[a]	465	**465**	465	–	–	–
AH-2	NMP + HCl[a]	486	487	**488**	492	528	528
	Blend + HCl[b]	nd	434	**437**	nd	nd	nd
AH-3	NMP + HCl[a]	466	467	**467**	478	–	–
	Blend + HCl[b]	nd	nd	439	nd	nd	nd
AH-4	NMP + HCl[a]	**424**	425	428	–	–	–
	Blend + HCl[b]	nd	nd	417; 435	nd	nd	nd
AH-5	NMP + HCl[a]	**425**	434	439	–	–	–
	Blend + HCl[b]	nd	nd	434	nd	nd	nd

Bold data indicates the most intense luminescence of compound.
* Not determined.
[a] $c = 1 \times 10^{-5}$ mol/l.
[b] Concentration = 1% of compound in PMMA.

blends were in the all cases significantly blue shifted in comparison with the ones observed in the solution. Photoluminescence spectra in NMP solution and in the blends of the compound **AH-2** are presented in Fig. 5c, as an example, whereas, the others are shown in Fig. 3S in Supporting Information. It was found that all compounds both in solution and in blend emitted blue light. Fig. 4S in Supporting Information shows the photographs of the photoluminescence of the compounds in NMP solution along with their PL in the blends under λ_{ex} = 366 nm. The PL ability of AH-1 and AH-5 films was tested. Both films emitted light with very low intensity (cf. Fig. 5d and e).

Relative PL intensity of the obtained compounds except for AH-3 was estimated in NMP solution in relation to rhodamine-B used as a standard. The emission spectra of rhodamine-B were recorded under the same experimental conditions as for investigated azines, that is, the same concentration (1×10^{-5} mol/l) and using the excitation wavelength corresponding to the most intense emission band of azine in NMP solution. For azines, relative PL intensity was found in the range of 98–437% in relation to emission intensity of rhodamine-B under the same excitation wavelength, concentration and solution (cf. Fig. 5f and Fig. 5S). The most intense and the lowest photoluminescence in NMP solution exhibited the compound AH-4 and AH-2, that is, 437% and 98% in relation to standard, respectively. Relative PL intensity of AH-1 and AH-5 was 238 and 213% compare to intensity of rhodamine-B, respectively.

In the investigations of optical properties, that is, absorption and emission in UV–vis range, the Stokes shifts could be analyzed. From a practical point of view large Stokes shift is desirable in order to avoid self-absorption of emitted light that reduces luminescence efficiency. The Stokes shifts values being collected in Table 5 were calculated for the most intense emission band of the studied compounds.

The highest difference between absorption and emission bands in NMP solution i.e. the biggest Stokes shift was found for the compound **AH-4**. It is worth to stress that for this compound the highest relative intensity of luminescence was found. In the case of blends the Stocks shifts were smaller than the ones for the compounds detected in solution.

3.2.3. Doping of azines

The effect of doping with HCl, TFA and $FeCl_3$ on optical properties of synthesized hydrazine derivatives was investigated in solution and in solid state. The spectral data from UV–vis and PL measurements after doping are collected in Tables 6 and 7, respectively.

On the first stage the solutions of compounds in NMP ($c = 1 \times 10^{-5}$ mol/l) and blends with PMMA were exposed to HCl vapor for the night [39]. The color of yellow solutions of compounds AH-1, AH-2, AH-3 disappeared, whereas blends of these compounds changed color from yellow to red (cf. Fig. 6).

No change was observed for the colorless solutions and blends of AH-4 and AH-5. Considering UV–vis spectra of the azines after doping the changes in the visible region were clearly observed (cf. Fig. 6b and Fig. 6S). In the case of azines with TPA units the intensity of this absorption band decrease and hypsochromic shift was found in NMP solution. In UV–vis spectra of AH-4 and AH-5 after doping also shift of λ_{max} to lower energy region was found, however, increase in intensity of this band is seen (cf. Fig. 6S). Considering UV–vis spectra of compounds in blends also hypsochromic shift of λ_{max} after doping was detected (cf. Table 3 and Fig. 3c). Moreover, in absorption spectra of azines with TPA structure small new band about 500 nm appeared. The PL spectra of hydrazine derivatives containing in their structure TPA moiety recorded after doping exhibited significant increase in PL intensity. Moreover, doping of these azines caused the bathochromic shift of λ_{em}. Almost opposite behavior of AH-4 and AH-5 after doping was found compare to the other azines. Fig. 6c presents PL spectra of AH-1 before and after doping in solution as example, whereas in Fig. 7S. are collected the PL spectra of the others azines. Doping the compounds in blend also increased their PL intensity but not so much as in solution and also shifted the λ_{em}, however, to the higher energy region. Fig. 6d presents PL spectra of AH-1 before and after doping in blend as example, whereas in Fig. 8S are presented the PL spectra of the others azines.

The next step of doping investigations concerns reversibility of protonation and oxidation of two azines with and without TPA moiety, that is, AH-1 and AH-5, respectively. Doping with TFA and $FeCl_3$ was carried out in CH_2Cl_2 solution and in thin film on glass substrate. The samples were protonated using TFA vapor and then neutralized with triethylamine (TEA). Similar to the neutralization with TEA, the intermediate obtained due to oxidation was reduced with hydrazide hydrate (N_2H_4). As seen in Fig. 7a

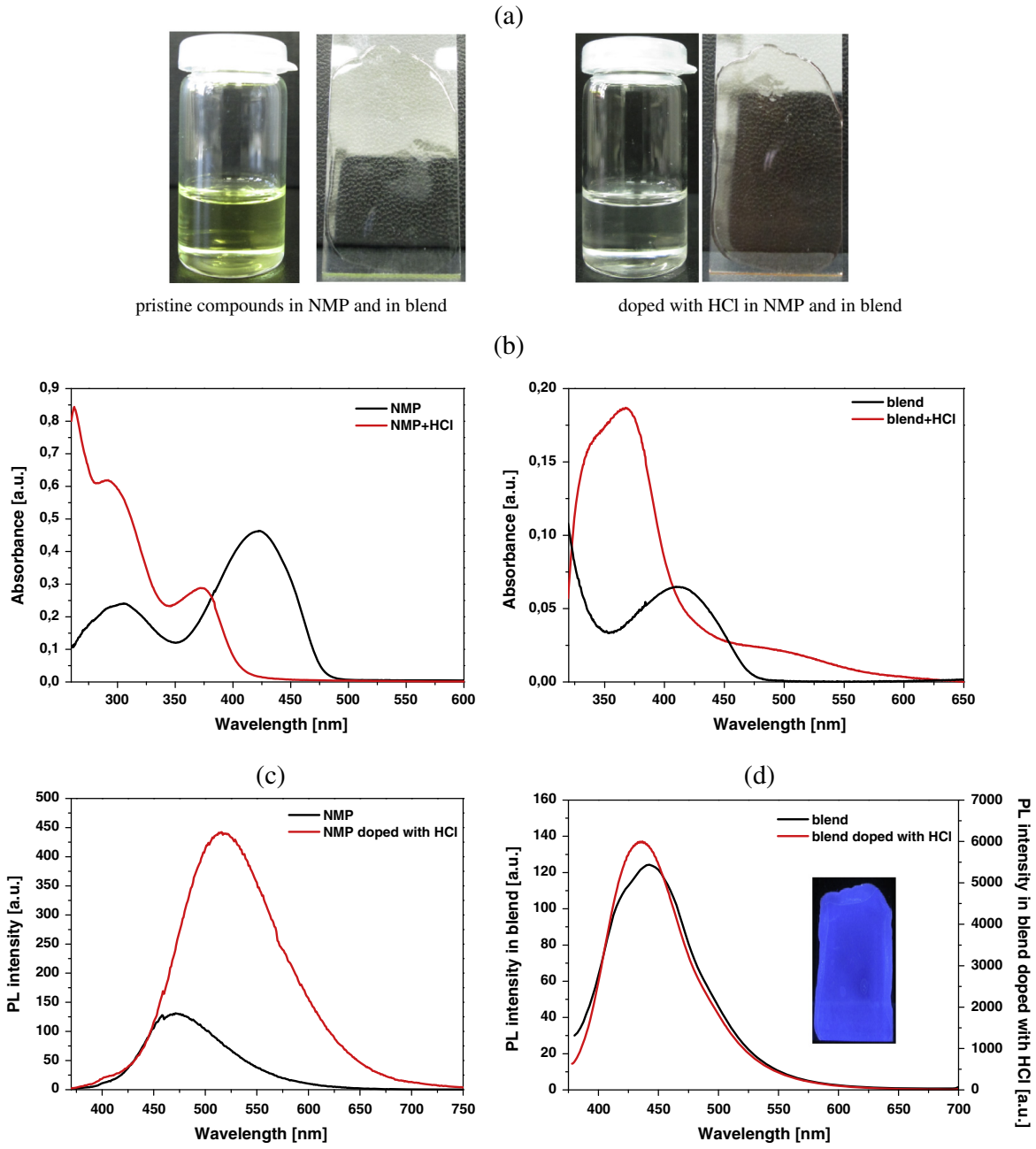

Fig. 6. (a) Photographs of AH-2 before and after doping with HCl in NMP solution and in blend, (b) absorption spectra of AH-3 in NMP solution and in blend before and after doping with HCl, (c) PL spectra of **AH-1** before and after doping with HCl in solution and in (d) blend λ_{ex} = 360 nm).

the protonation of AH-1 with TFA in solution results in appearance of new absorption band with λ_{max} at 498 nm (cf. Table 6) and change in solution color was observed from yellow to dark yellow.

Thus, the AH-1 doped with TFA exhibited different behavior compare to doping with HCl where a yellow color of solutions disappeared after HCl protonation. The oxidation with $FeCl_3$ results in a 128 nm bathochromic shift in absorbance (cf. Table 6 and Fig. 7a) and red color of AH-1 solution was seen. In the case of azine AH-5 after protonation with TFA the lack of changes in UV–vis spectrum was observed (cf. Fig. 7b). Whereas, after doping AH-5 with $FeCl_3$ broadening of absorption band is seen and color of solution became yellow. The resulting intermediates can subsequently be deprotonated with TEA or reduced with hydrazine hydrate to regenerate the neutral AH-1 and AH-5. It is noteworthy that the absorbance spectrum of the neutral azines after having been exposed to TFA/TEA and $FeCl_3/N_2H_4$ cycles is identical to that of pristine samples. Next the doping/dedoping process in thin film from AH-1 was examined. The films color changed from yellow to red or orange (cf. Fig. 7c). Thus, it was found that the investigated diimines are hydrolytically stable and addition of oxidant does not result in decomposition of azines.

3.3. DFT calculations

The quantum theoretical calculations using density functional theory (DFT), with an exchange correlation hybrid functional B3LYP and the basis 6-31G(2d,p) for carbon, nitrogen and 6-31G for hydrogen atoms were performed with use of Gaussian 09 program [40]. The geometries of the studied compounds were simulated and optimized in vacuum and no imaginary frequencies

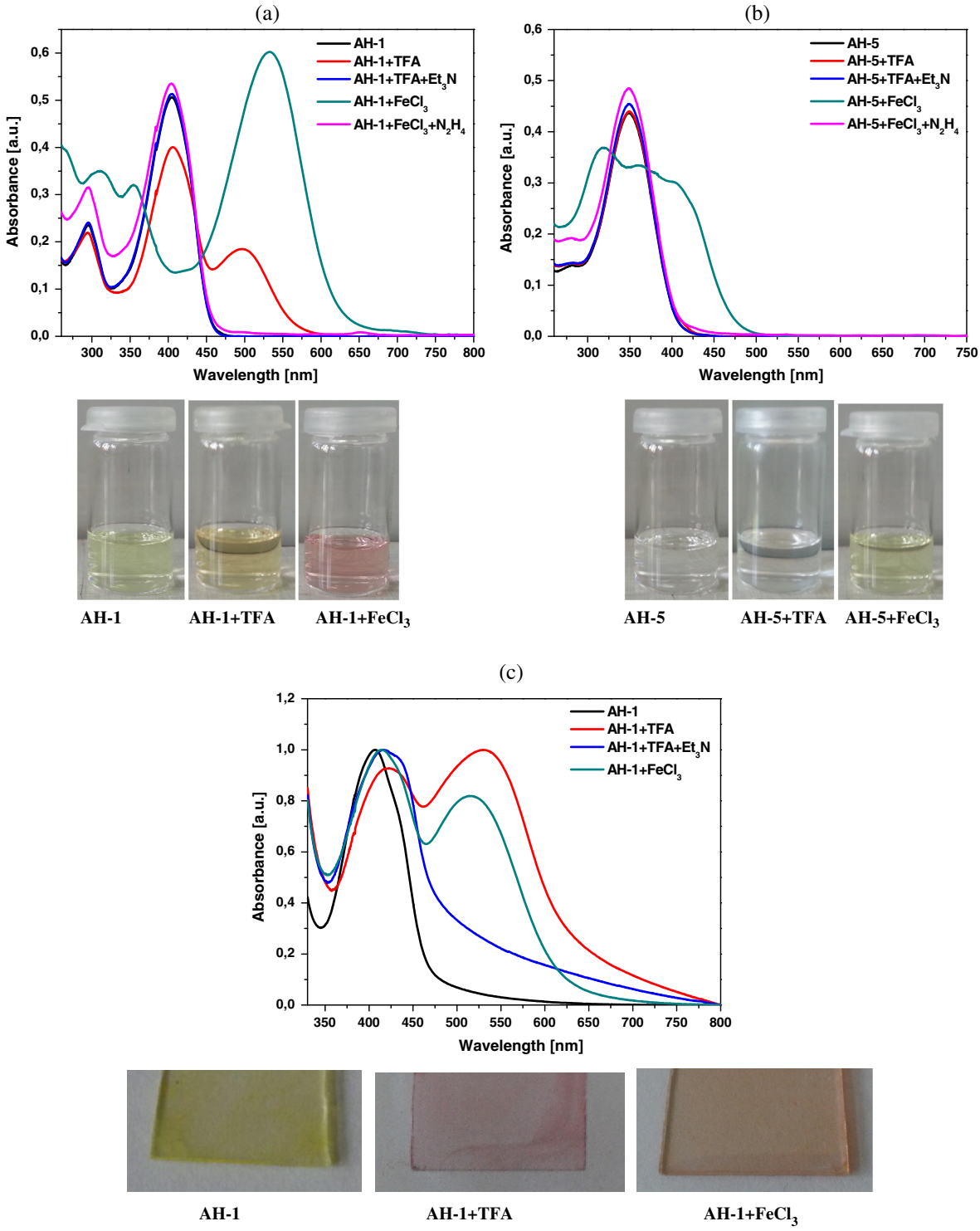

Fig. 7. UV–Vis spectra of **AH-1** (a) and **AH-5** (b) in CH_2Cl_2 after doping and dedoping with TFA/Et_3N and $FeCl_3/N_2H_4$, and (c) **AH-1** as thin film after doping and dedoping with TFA/Et_3N and protonation with $FeCl_3$.

were found for any of these species, computed without symmetry restriction, by vibrational analysis. Based on the optimized geometries the energy and electronic distribution of molecular frontier orbitals were calculated in dichloromethane solution and the solvent effect was introduced by PCM model for comparison with experimental electrochemical potentials. The frontier orbitals are of extreme importance for the evaluation of molecular reactivity. As much is negative the energy of the Highest Occupied Molecular Orbital (HOMO), more susceptible is the molecule to donate electrons and, consequently, higher is the tendency to suffer oxidation. A similar argument can be used to interpret the tendency of a given molecule in suffer reduction, on the basis of the energy of the Lowest Unoccupied Molecular Orbital (LUMO). The contours of HOMOs and LUMOs are depicted in Fig. 8.

HOMO orbitals in these compounds, except AH-3, are localized on the conjugated double bonds system comprising the aromatic rings and in its neighborhood (—CH=N—N=CH—), indicating that the oxidation process would have to happen primarily in this

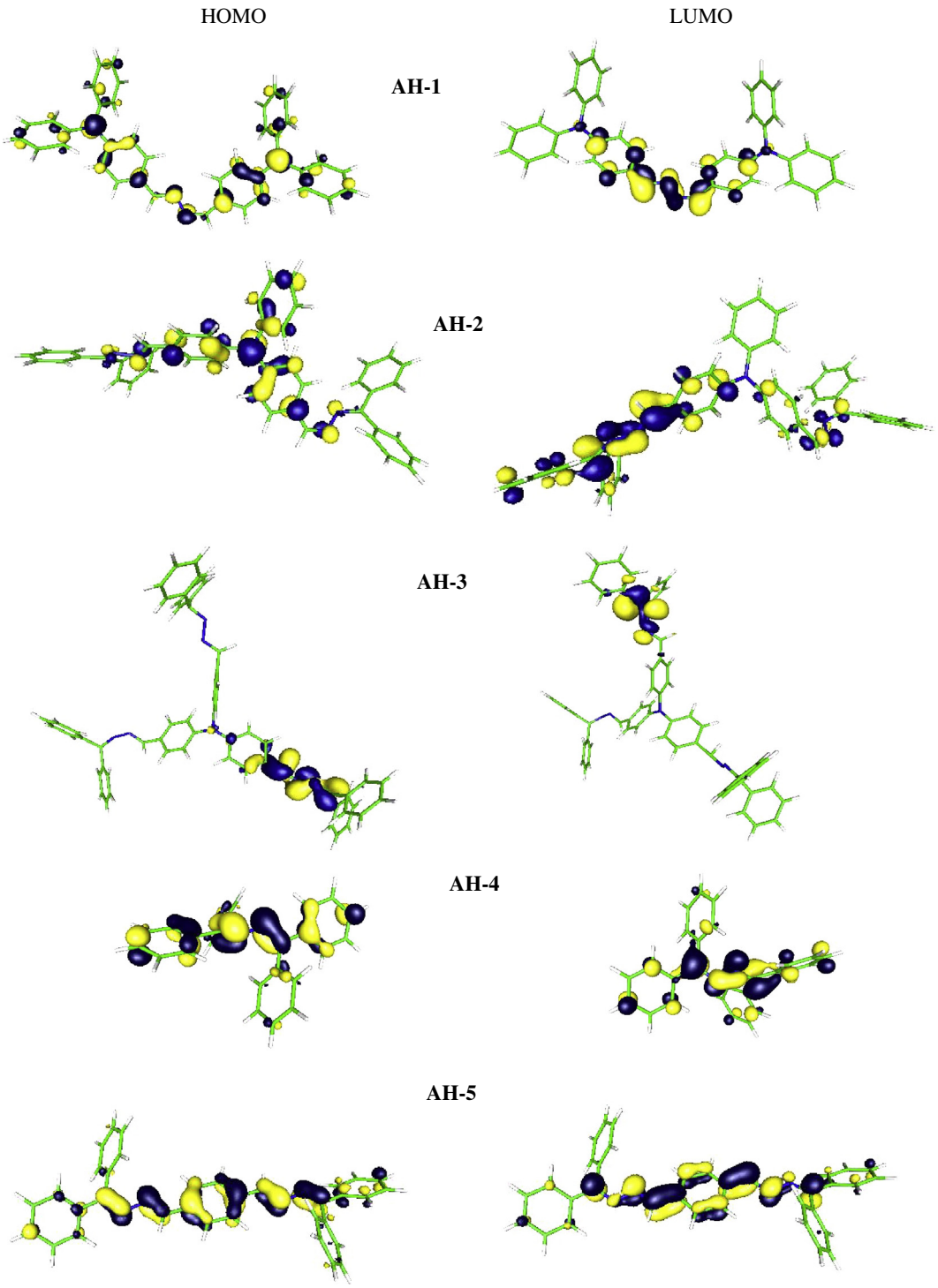

Fig. 8. HOMO and LUMO contours of investigated azines.

region. This corresponds to the calculations of electronic density, which indicate that this region has the highest density of negative charge (cf. Fig. 9S). LUMOs are localized on nonbonding (p_z) orbitals excluding double bonds and aromatic parts of the molecules. In the case of AH-3 HOMO and LUMO are localized on the one azine fragment of molecule. The calculations of the Mulliken charge are widely used to identify the set of atoms that has a greater tendency to undergo oxidation, based on the distribution of the orbitals HOMO on the molecule. The results indicate that this =N—N= group has the more negative charge (−0.634) compared with other two diimine parts (−0.523 and −0.480) in this molecule demonstrating that the oxidation would occur most probably on this part of molecule; naturally LUMO is localized on the most positive azine fragment. The calculated frontier orbital energy levels are shown in Table 8.

The HOMO energies ranged from −6.22 to −5.03 eV. The oxidation process involves the removal of an electron from the HOMO, thus AH-1 compound with highest HOMO energy level would be most readily to donate the electron. This can be explained by the fact that in this molecule strong π- π conjugation effect is pre-

sented (Fig. 9) leading to a rise in HOMO energy. Incorporation of phenyl group into molecule as one can see when comparing AH-4 and AH-5 compounds leads to a rise in HOMO energy. The introduction of phenyl group in compound AH-2 and AH-3 results in increasing of HOMO energy while the terminal triphenylamine moiety plays meaningful role in decreasing the energy.

The LUMO energies varied from −2.83 to −1.93 eV and as one can see from Table 8 the compositions of the molecules have less impact on the energies of LUMOs. The HOMO–LUMO gap is an important stability index and a large energy gap implies high stability for the molecule. Therefore AH-4 characterizes the highest stability (E_g = 4.03 eV) and E_g = 3.03 eV calculated for AH-3 suggests lowest stability. The relatively high gap in the AH-4 compound is connected with their comparatively simple molecular structure composed of only four benzene rings.

3.4. Electrochemical properties

In order to verify the results of theoretical calculations concern HOMO, LUMO energies electrochemical measurements were carried out. The electrochemical properties of film coated on a ITO disk prepared from the obtained compounds were investigated by cyclic voltammetry (CV) in MeCN solution (containing Bu_4NPF_6 as the supporting electrolyte). According to measured oxidation and reduction potentials, values of HOMO–LUMO bands were calculated. The electrochemical data are collected in Table 8. Fig. 9 presents the obtained voltammograms of azines AH-3 and AH-5 as example.

Table 8
Theoretical values of HOMO, LUMO and energy band gap and electrochemical data of azines.

	AH-1	AH-2	AH-3	AH-4	AH-5
E_{ox1} (V)	0.57	0.77	0.72	1.38	1.30
E_{ox2} (V)	0.84	–	0.85	–	–
E_{red1} (V)	−2.23	−2.33	−2.51	−2.35	−1.95
E_{red2} (V)	–	–	–	–	−2.11
$E_{ox,onset}$ (V)	0.40	0.53	0.59	1.13	1.07
$E_{red,onset}$ (V)	−2.14	−2.09	−2.16	−2.11	−1.82
E_{HOMO} (eV)	−5.25	−5.37	−5.43	−5.94	−5.88
E_{LUMO} (eV)	−2.68	−2.73	−2.66	−2.71	−3.00
E_g (eV)	2.57	2.64	2.77	3.23	2.88
E_{HOMO} (eV) DFT	−5.03	−5.20	−5.22	−6.22	−6.13
E_{LUMO} (eV) DFT	−1.93	−2.11	−2.19	−2.19	−2.81
E_g (eV) DFT	3.10	3.09	3.03	4.03	3.32

$E_{HOMO} = -4.82 - E_{ox,onset}$.
$E_{LUMO} = -4.82 - E_{red,onset}$.
$E_g = E_{ox,onset} - E_{red,onset} = E_{HOMO} - E_{LUMO}$.

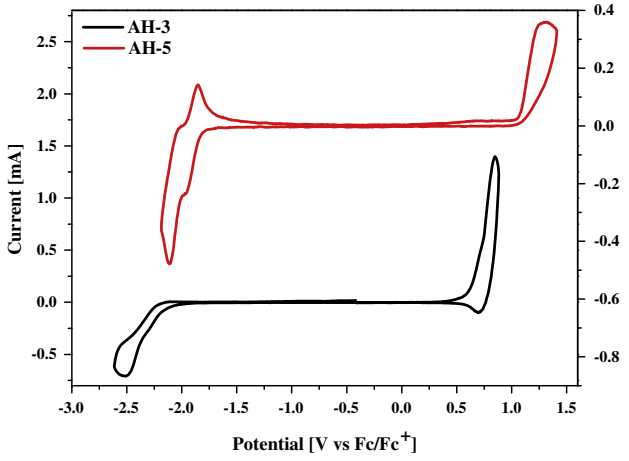

Fig. 9. Cyclic voltammograms of AH-3 and AH-5 film coated on a ITO disk (scan rate 50 mV s^{-1}, electrolyte 0.1 M Bu_4NPF_6 in MeCN).

All azines containing triphenylamine units (AH-1–AH-3) exhibited quasi-reversible oxidation process with potential onset ($E_{ox,onset}$) in the range 0.40 to 0.59 V. This results from the creation of cation radical in triphenylamine unit [19,41]. For the other two compounds (AH-4 – AH-5), the oxidation process is irreversible and oxidation peak is shifted to a higher potential ($E_{ox,onset}$ in the range 1.07–1.13 V). Reduction was observed for all azines, but only AH-5 showed a fully reversible two-electron process with onset potential at −1.82 V. Azines containing aromatic linkage between imine bonds were harder to reduced (onset potential in the range −2.09 to −2.16 V). The HOMO energy level of azines was in the range of −5.25 to −5.94 eV. Azines containing triphenylamine units exhibited a significantly higher value of the HOMO energy level, and it slightly decreased with increasing number of imine bonds attached to triphenylamine unit. Azine AH-4, with phenyl linkage between imine bonds exhibited the lowest HOMO lever (−5.94 eV). Azine AH-5 exhibited the lowest LUMO level (−3.0 eV), since other compounds exhibited similar value of LUMO levels, in the range −2.66 to −2.73 eV. This is in good agreement with DFT calculations, which shows the lowest energy of LUMO for AH-5, HOMO for AH-4 and the highest energy band gap for AH-4. However the values of calculated and measured energies are usually slightly higher, it is due to a various effects in films and solutions.

4. Conclusions

Five hydrazine derivatives were obtained and investigated by DSC, TGA, UV–vis, PL, CV techniques. Moreover, electronic distribution of their molecular frontier orbitals were theoretically calculated using density functional theory (DFT). DSC study revealed that these compounds exhibited behavior of molecular glasses. The highest T_g = 98 °C exhibits compound prepared from 4,4′-diformyltriphenylamine and benzophenone hydrazone. The replacement in compound of TPA unit (AH-2) by phenyl ring (AH-5) decreased the T_g but did not effect on decomposition temperature, however, significantly reduced residue at 800 °C. Azines with TPA structure showed intense absorption band in the visible range with maximum at 404–422 nm. Absorption of azines without TPA was hypsochromically shifted. All azines emitted blue light both in solution and in solid state as blend with PMMA, however, the most intense emission was detected for compound without imine linkages. Doping of compounds with HCl changed both their absorption in UV–vis range and PL properties, that is shifted λ_{max} and increased intensity of emitted light except for azines without TPA unit (protonation reduced PL intensity). The obtained azine with TPA units repeated exposure to concentrated acids and $FeCl_3$ demonstrate hydrolytic and chemical oxidative resistance. Investigated hydrazine derivatives undergo electrochemical oxidation and reduction processes. However, oxidation process of azines with and without TPA was quasi-reversible and irreversible, respectively, whereas, reduction process was reversible only in case of AH-5. Compound with and without TPA moieties can be treated as p-type semiconductor with HOMO level between −5.25 and −5.43 eV and as n-type semiconductor with LUMO level between −2.68 and −3.00 eV (relative to vacuum level), respectively. Considering the E_g the lowest (2.57–2.77 eV) was found for azines with TPA moieties.

Acknowledgments

Calculations have been carried out using resources provided by Wroclaw Centre for Networking and Supercomputing (http://wcss.pl), Grant No. 18. M. Grucela-Zajac would like to acknowledge

a financial support from Mobility Plus Programme financed by MNiSW.

Appendix A. Supplementary material

Supplementary data associated with this article can be found, in the online version, at http://dx.doi.org/10.1016/j.optmat.2014.07.013.

References

[1] J. Roncali, P. Leriche, A. Cravino, Adv. Mater. 19 (2007) 2045–2060.
[2] A. Pron, P. Gawrys, M. Zagorska, D. Djurado, R. Demadrille, Chem. Soc. Rev. 39 (2010) 2577–2632.
[3] B. Lucas, Th. Trigaud, Ch. Videlot-Ackermann, Polym. Int. 61 (2012) 374–384.
[4] Y. Shirota, J. Mater. Chem. 10 (2000) 1–25.
[5] Y. Shirota, J. Mater. Chem. 15 (2005) 75–93.
[6] S. Plante, O. Palato, A. Lebel, J. Soldera, Mater. Chem. C 1 (2013) 1037–1042.
[7] N. Bakken, J.M. Torres, J. Li, B.D. Vogt, Soft Matter 7 (2011) 7269–7273.
[8] H. Dong, H. Zhu, Qi Meng, X. Gong, W. Hu, Chem. Soc. Rev. 41 (2012) 1754–1808.
[9] J. Safari, S. Gandomi-Ravandi, Synth. Comm. 41 (2011) 645–651.
[10] R. Cohen, B. Rybtchinski, M. Gandelman, L.J.W. Shimon, J.M.L. Martin, D. Milstein, Angew. Chem. 115 (2003) 1993–1996.
[11] A.I. Khodai, P. Bertrand, Tetrahedron 54 (1998) 4859–4872.
[12] D.D. Choytun, L.D. Langlois, T.P. Johansson, C.L.B. Macdonald, G.W. Leach, N. Weinberg, J.A.C. Clyburne, Chem. Commun. (2004) 1842–1843.
[13] R. Centore, C. Garzillo, J. Chem. Soc. Perkin Trans. 2 (1997) 79–84.
[14] M. Moreno-Manas, R. Pleixats, R. Andreu, J. Garin, J. Orduna, B. Villacampa, E. Levillain, M. Salle, J. Mater. Chem. 11 (2001) 374–380.
[15] A. Iwan, P. Rannou, H. Janeczek, M. Palewicz, A. Hreniak, P. Bilski, F. Oswald, D. Pociecha, Synth. Met. 160 (2010) 859–865.
[16] W. Tang, Y. Xiang, A. Tong, J. Org. Chem. 74 (2009) 2163–2166.
[17] R. Wei, P. Song, A. Tong, J. Phys. Chem. C 117 (2013) 3467–3474.
[18] J. Kulhanek, F. Bures, W. Kuznik, I.V. Kityk, T. Mikysek, A. Ruzicka, Chem. Asian J. 8 (2013) 465–475.
[19] M. Grigoras, L. Vacareanu, T. Ivan, A.M. Catargiu, Dyes Pigm. 98 (2013) 71–81.
[20] B. Krishnakumar, M. Swaminathan, Catal. Commun. 16 (2011) 50–55.
[21] M. Thelakkat, Macromol. Mater. Eng. 287 (2002) 442–461.
[22] Z. Ning, H. Tian, Chem. Commun. (2009) 5483–5495.
[23] A. Iwan, D. Sek, Prog. Polym. Sci. 36 (2011) 1277–1325.
[24] Y. Fu, H. Li, W. Hu, Eur. J. Org. Chem. (2007) 2459–2463.
[25] D. Sek, M. Siwy, K. Bijak, M. Grucela-Zajac, J.G. Malecki, K. Smolarek, L. Bujak, S. Mackowski, E. Schab-Balcerzak, J. Phys. Chem. A 117 (2013) 10320–10332.
[26] H. Niu, J. Cai, P. Zhao, Ch. Wang, X. Bai, W. Wang, Dyes Pigm. 96 (2013) 158–169.
[27] D. Sek, K. Bijak, M. Grucela-Zajac, M. Filapek, L. Skorka, M. Siwy, H. Janeczek, E. Schab-Balcerzak, Synth. Met. 162 (2012) 1623–1635.
[28] D. Sek, M. Lapkowski, H. Dudek, K. Karon, H. Janeczek, B. Jarzabek, Synth. Met. 162 (2012) 1046–1051.
[29] E. Schab-Balcerzak, E. Grabiec, M. Kurcok, J. Phys. Chem. A 113 (2009) 1481–1488.
[30] E. Schab-Balcerzak, M. Grucela-Zajac, M. Krompiec, H. Janeczek, M. Siwy, D. Sek, Synth. Met. 161 (2011) 2268–2279.
[31] M. Grucela-Zajac, M. Filapek, L. Skorka, J. Gasiorowski, E.D. Glowacki, H. Neugebauer, E. Schab-Balcerzak, Mater. Chem. Phys. 137 (2012) 221–234.
[32] K. Bijak, H. Janeczek, M. Grucela-Zajac, E. Schab-Balcerzak, Opt. Mater. 35 (2013) 1042–1050.
[33] M. Grucela-Zajac, K. Bijak, S. Kula, M. Filapek, M. Wiacek, H. Janeczek, L. Skorka, J. Gasiorowski, K. Hingerl, N.S. Sariciftci, N. Nosidlak, G. Lewinska, J. Sanetra, E. Schab-Balcerzak, J. Phys. Chem. C 118 (24) (2014) 13070–13086.
[34] L.J. Bellamy, The Infrared Spectra of Complex Molecules, John Wiley and Sons Inc., New York, 1975.
[35] G. He, Y. Li, J. Liu, Y. Yang, Appl. Phys. Lett. 80 (2002) 4247–4249.
[36] A.K. Nedeltchev, H. Han, P.K. Bhowmik, Tetrahedron 66 (2010) 9319–9468.
[37] M. Granström, M. Berggren, D. Pede, O. Inganäs, M.R. Andersson, T. Hjertberg, O. Wennerström, Supramol. Sci. 4 (1997) 27–34.
[38] A. Bolduc, L. Rivier, S. Dufresne, W.G. Skene, Mater. Chem. Phys. 132 (2012) 722–728.
[39] H. Niu, P. Luo, M. Zhang, L. Zhang, L. Hao, J. Luo, X. Bai, W. Wang, Eur. Polym. J. 45 (2009) 3058–3071.
[40] M.J. Frisch, G.W. Trucks, H.B. Schlegel, G.E. Scuseria, M.A. Robb, J.R. Cheeseman, G. Scalmani, V. Barone, B. Mennucci, G.A. Petersson, H. Nakatsuji, M. Caricato, X. Li, H.P. Hratchian, A.F. Izmaylov, J. Bloino, G. Zheng, J.L. Sonnenberg, M. Hada, M. Ehara, K. Toyota, R. Fukuda, J. Hasegawa, M. Ishida, T. Nakajima, Y. Honda, O. Kitao, H. Nakai, T. Vreven, Jr.J.A. Montgomery, J.E. Peralta, F. Ogliaro, M. Bearpark, J.J. Heyd, E. Brothers, K.N. Kudin, V.N. Staroverov, R. Kobayashi, J. Normand, K. Raghavachari, A. Rendell, J.C. Burant, S.S. Iyengar, J. Tomasi, M. Cossi, N. Rega, J.M. Millam, M. Klene, J.E. Knox, J.B. Cross, V. Bakken, C. Adamo, J. Jaramillo, R. Gomperts, R.E. Stratmann, O. Yazyev, A.J. Austin, R. Cammi, C. Pomelli, J.W. Ochterski, R.L. Martin, K. Morokuma, V.G. Zakrzewski, G.A. Voth, P. Salvador, J.J. Dannenberg, S. Dapprich, A.D. Daniels, O. Farkas, J.B. Foresman, J.V. Ortiz, J. Cioslowski, D.J. Fox, Gaussian Inc, Gaussian 09, Revision A.1, Wallingford CT, 2009.
[41] Y.-Ch. Kung, S.-H. Hsiao, Polym. Chem. 2 (2011) 1720–1727.